

Some numerical assessments on intergranular crack propagation in polycrystals. Application to γ -TiAl

D. Geoffroy ^{1,2}, J. Crépin ², E. Héripré ³, A. Roos ¹

¹ DMSM/MNU, ONERA, France

² Centre des Matériaux, MINES-ParisTech UMR CNRS 7633, France

³ LMS, Ecole Polytechnique ParisTech UMR CNRS 7649, France

dominique.geoffroy@onera.fr

ABSTRACT

This work presents a numerical study of the intergranular crack propagation behavior of γ -TiAl. For this purpose, finite element simulations using remeshing techniques and crystal plasticity are carried out on a bidimensional γ -TiAl polycrystal. In order to evaluate the influence of crystal orientations, ten different random orientations are generated and used on the same finite element polycrystal mesh. First the force-displacement curves are analysed to show that the crystal orientations influence significantly the material's global response. Then, the paths taken by the crack in the different polycrystals are investigated, but they show that crystal orientations do not seem to have a great influence on them.

INTRODUCTION

The thrust-to-weight ratio has always been a crucial criterion in the design of aircraft engines because of its influence on the turbine's efficiency and gas consumption. Since an important part of the aircraft weight is in the engine, many studies have been carried out in order to find new materials for that specific application. Among them, titanium aluminides seem very promising because of their excellent properties at high temperatures. However, the widespread use of this material is still quite limited by its low fracture toughness at room temperature and its mechanical properties' high sensitivity on the microstructure. Hence, the microstructural properties need to be taken into account when investigating its mechanical response.

Many studies have been carried out on these alloys during the last decades [1, 2, 3]. Among them, Héripré *et al.* [4] developed a coupling method between numerical simulations and experimental studies to identify the parameters of the crystal plasticity constitutive law. Finite element (FE) simulations can now be conducted on this material, as done by Héripré [5], Kabir *et al.* [6], Roos *et al.* [7] and Roters *et al.* [8]. Also, Simkin *et al.* [9] showed that the crack initiation and propagation in γ -TiAl was

correlated to the activation of twinning mechanisms and many crack propagation criteria were developed. The cracks either propagate on the twin planes or the grain boundaries, depending on the misorientation between the grains' crystals, the grain boundary's orientation and the applied load. These criteria can statistically predict for γ -TiAl (Ti-48Al-2C-2Nb) the tendency for a crack to propagate along the grain boundary or inside the grain. Finally, Werwer *et al.* [10] simulated crack propagation in homogenized lamellar TiAl in three dimensions by using cohesive zone elements (CZE).

The general framework of this project is the study by FE and CZE of crack propagation in γ -TiAl considering the effects of crystal plasticity. Following [9, 11, 12], two crack propagation mechanisms are modeled : intergranular (i.e. along the grain boundaries) and intragranular on the twin planes. Previously [13], a numerical study was carried out to approximate the parameters of the cohesive zone models (CZM) for both mechanisms. Now that these are known, CZE and crystal plasticity can be coupled in three-dimensional polycrystal FE computations.

However, prior to these simulations with multiple crack mechanisms, the intergranular crack propagation alone is studied and is the topic of this work. Since the crack path is unknown at the beginning of the computation, a remeshing process is used to insert CZE during the simulation. First, the FE mesh employed and the precrack inserted in the mesh are presented. Then, the material models, the remeshing process and the boundary conditions are shown. Finally, the influence of the crystal orientations on the crack path and the force-displacement behavior is evaluated.

FE MESH , MATERIAL, CONSTITUTIVE LAWS, REMESHING PROCESS AND BOUNDARY CONDITIONS

This section presents the different parameters of the model. First, the mesh used for the FE computations is presented. Then, the deformation mechanisms of the material are described, followed by the material's constitutive law and the CZM parameters. The remeshing process employed in order to add CZE to the mesh during the simulation is afterwards exhibited. Finally, the loading and boundary conditions are presented.

FE Mesh

A bidimensional mesh of 102 grains of $1 \times 1 \text{ mm}^2$ was built for the FE simulation using the method developed by St-Pierre *et al.* [14]. It is presented on Figure 1. With this specific mesh, ten different simulations are performed using different crystal orientations to analyse its influence on the intergranular crack propagation. The crystal orientations have been randomly chosen for the ten simulations.

A precrack is inserted between two grains on the left side of the polycrystal. CZE are then added on the grain boundaries next to the precrack to allow the initial crack propagation. The precrack is shown in Figure 2(b).

Material and constitutive laws

The material studied is γ -TiAl which has a slightly quadratic FCC $L1_0$ structure. Three plastic deformation mechanisms are available in this material [15]: ordinary dislocations $\langle 1\bar{1}0 \rangle \{111\}$, superdislocations $\langle 01\bar{1} \rangle \{111\}$, and twinning $1/6 \langle 11\bar{2} \rangle \{111\}$. The twins are modeled as one-way slip even though they represent physically a different mechanism.

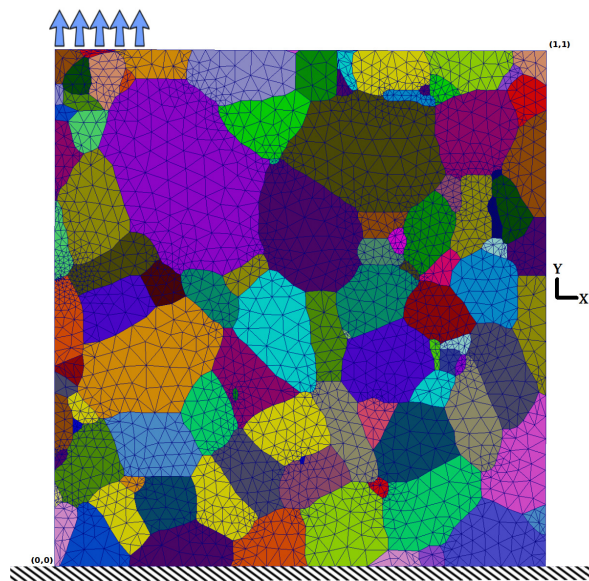


Figure 1. Initial FE mesh used for the intergranular crack propagation simulations.

The bulk material's elements are modeled using an elasto-visco plastic constitutive law with linear hardening [16, 17]. Since a 2D mesh is used, plane strain conditions are imposed. For the grains on the top of the mesh, anisotropic elasticity is used in order to limit the plastic strain induced by the boundary conditions. The hardening matrix \mathbf{h} is supposed diagonal (with the diagonal terms $h_0 = 1230$ MPa self-hardening for all the slip systems, determined by Gélébart [18]). Cross-slip hardening is not considered since it is unknown for γ -TiAl. The critical resolved shear stresses τ_0 used have been determined via in-situ strain field measurements from Gélébart [18] and are $\tau_{0,ordinary}=250$ MPa, $\tau_{0,super}= 333$ MPa, and $\tau_{0,twin}=250$ MPa.

The Elastic tensor is taken quadratic and was measured experimentally by [19] on a monocrystal. Using Voigt's notation, the parameters are $C_{11}=C_{22}=183$ GPa,

$C_{12}=C_{21}=C_{13}=C_{31}=C_{23}=C_{32}=74.1$ GPa, $C_{33}=178$ GPa, $C_{44}=C_{55}=105$ GPa, $C_{66}=78.4$ GPa. All other elastic constants are 0.

The CZE are modeled using a formulation developed by Lorentz [20] and a CZM from Mi [21] with an initial perfect adhesion. The jump in the displacement field δ at the cohesive interface is then linearly linked to the stress until it reaches a critical value δ_N . Meanwhile, a scalar damage parameter λ takes into account the irreversibility of the damage process : $\lambda = \max_{\text{time}}(\delta/\delta_N)$. It is presented in Figure 2(a) and the parameters $\sigma_{Nmax} = 800$ MPa and $\delta_N = 24$ μm are taken from previous numerical studies. These parameters are not the exact ones, but are sufficient to describe the competition between the intragranular and intergranular crack propagation mechanisms [13]. The use of this CZE fomulation imposes a quadratic interpolation on the whole mesh.

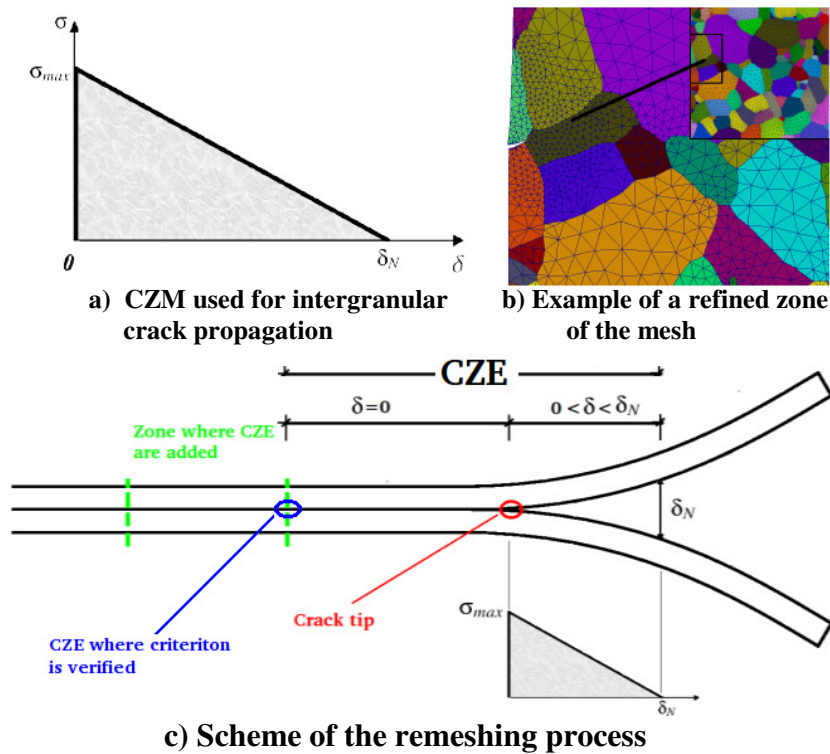


Figure 2. CZM used, an adaptive mesh example and a scheme of the remeshing process.

Remeshing Process

A remeshing process is used in order to refine the mesh around the crack tip and to add new CZE during the FE simulations. In this model, since all the grain boundaries are considered as potential crack paths the remeshing procedure can only add CZE

between the grains. At the end of every time increment, the damage parameter λ of the CZM is used as a remeshing criterion. It is evaluated on the last CZE of every crack front to verify the location of the crack tip, as shown on Figure 2 c). For every crack front, $\lambda=0$ (i.e. $\delta=0$ mm) implies that the crack tip is not situated on its last CZE. On the opposite, if $\lambda>0$ (i.e. $\delta >0$ mm) in the last CZE of the crack front, a crack tip is located on it and therefore the crack propagation is limited by the discretisation of the crack by the CZE on the crack path. The remeshing process is therefore triggered on the crack front where the criterion was met.

The remeshing process adds new CZE on the potential crack path within a radius of 0.03 mm where the remeshing criterion was met. Meanwhile, all the bulk material elements within a radius of 0.1 mm of the crack tip are refined in order to have a fine mesh (around 5 μm instead of 30 μm between two nodes) around the new crack tip.

Once the remeshing procedure is over, the mechanical fields from the last converged increments are transferred to the new mesh. For the nodal fields, the position of the nodes on the new mesh are used to interpolate the fields from the last FE solution in the last mesh used. A special procedure is employed to ensure that the fields transferred around the crack are on the same side of the lips before and after the transfers. For the integration points (IP) fields, the closest IP in the last mesh and in the same grain is used to copy the fields over to the IP in the new mesh.

After transferring the fields, the last time increment is computed again to ensure that enough CZE were added on the crack fronts. If it is not the case, the remeshing procedure is triggered again and loops until enough CZE are added on every crack front.

Boundary conditions

A monotonic displacement ranging linearly from 0 to 10 mm in 1000 s is applied on all the nodes on the top of the polycrystal where $x<0.2$ mm. Simultaneously, all the nodes on the bottom have fixed 0 mm displacements in both directions. The boundary conditions used in the simulation are shown in Figure 1. Also, it is important to note that the imposed displacements do not ensure a stable crack growth and therefore rigid modes appear when the crack reaches the limit of the polycrystal.

RESULTS AND ANALYSIS OF POLYCRYSTAL FE SIMULATIONS

The FE simulations were carried out on ten polycrystals with different crystal orientations. Depending on the polycrystal, between 19 and 45 adaptive meshes were needed. Also, for some polycrystals, as the damage started, the remeshing process was triggered continuously until the crack reached the outer end of the polycrystal. Therefore, no data is available for these polycrystals during the fracture process because of the crack propagation's instability. This happened to the polycrystals where an important amount of plasticity was present before the fracture process.

First, the analysis is performed on the force-displacement behavior of the polycrystals. Then, the path taken by the crack is investigated. Both analyses are performed to determine if the crystal orientations influence significantly the material's mechanical response.

Force-Displacement analysis

The force-displacement curves have been analysed for the ten microstructures studied and are presented on Figure 3. Even if a considerable number of grains has been used in the model, it is interesting to note that the grain orientations have a great influence on the global force-displacement behavior. Between polycrystals 8 and 9, the force applied at the beginning of the crack propagation is twice as important. This shows that the stress state is locally different between the ten polycrystals and therefore, the plastic strain also is different. If the slip systems around the crack tip are oriented in a favorable way, plasticity will first be triggered which will postpone the damage evolution. On the opposite, if the only way to accommodate the stress is via the elastic strain, the local stress increases significantly and therefore triggers the damage process first. This explains why polycrystals 3, 4 and 9 have almost no data available after the beginning of the fracture process. For these, the crack propagation was first stabilised by the local hardening around the crack tip until the stress increased sufficiently to propagate the crack on the first grain boundary. Then, the crack continued to propagate up to the next grain boundaries where the slip systems were not oriented in order to favor plasticity. Therefore the crack propagated quickly and numerical instabilities were noted.

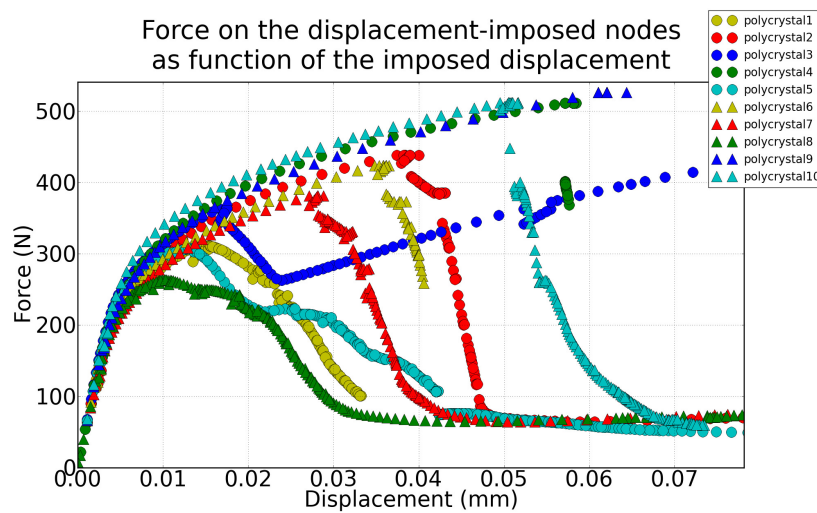


Figure 3. Force-displacement curves of the ten bicrystals

Polycrystal 3 has a different behaviour from the others. It is the only polycrystal where, after the damage processed started, the applied force increased. For this polycrystal, when the damage was initiated, the crack propagated up to the next grain

boundary. However, the slip systems around the new crack tip's position were oriented in a way that, in order to open the crack lips, an important amount of plasticity was needed. This phenomenon stopped the crack propagation, until the local stress state was high enough to propagate the crack.

Crack Path analysis

Two different crack paths have been found during the FE simulations performed on the ten polycrystals. They are both identical, except for one grain boundary. The two crack paths are shown in Figure 4.

From these first results, the crystal orientations do not seem to influence significantly the crack path. It seems that the path taken by the crack often favors mode I opening. In order to correctly evaluate the effect of the crystal orientations on the crack path, more data is needed. So far, only one geometry has been used. Hence, the effect of the grain boundary's orientations which may highly influence the crack path cannot be evaluated accurately. Further work shall provide more information on this topic.

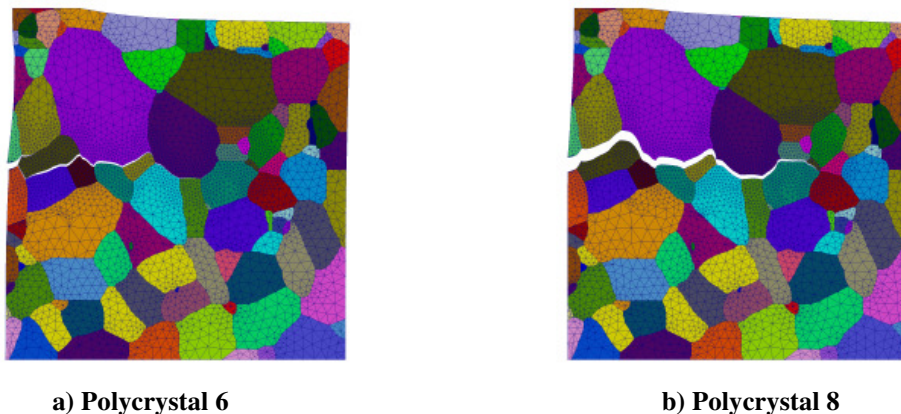


Figure 4. Crack path in polycrystals 6 and 8 at $t = 4.07$ s.

CONCLUSION

FE simulations were carried out on γ -TiAl in order to evaluate its intergranular crack propagation behavior. A bidimensional polycrystal was meshed and different crystal orientations were applied to evaluate their effects on the fracture toughness and the crack path. It was shown that the fracture toughness varies significantly when the crystal orientations are modified. Meanwhile, although the behavior of the whole polycrystal is very different, the crystal orientations do not seem, for a fixed mesh, to have a significant influence on the crack path.

A deeper investigation is however needed to accurately find the influence altogether of the crystal orientations and grain boundaries normals. Further work is also needed to

take into account the intragranular fracture mechanisms [22] in the FE simulations and therefore special attention must be given to the remeshing process needed to explicitly discretise the intergranular crack planes during the FE simulation. Finally, both crack propagation mechanisms should be considered simultaneously in a 3D polycrystal FE simulation with an experimental results comparison.

REFERENCES

1. Fujiwara, T., Nakamura, A., Hosomi, M., Nishitani, S.R., Shirai, Y., Yamaguchi, M. (1990) *Phil. Mag.* **A61(4)**, 591-606.
2. Umeda, H., Kishida, K., Inui, H., Yamaguchi, M., (1997), *Mat. Sc. Eng.* **A239-240**, 336-343.
3. Yamaguchi, M., Inui, H., Yokoshima, S., Kishida, K., Johnson, D.R. (1996), *Mater. Sc. and Eng* **A213**, pp. 25-31, 1996.
4. Héripré, E. (2006) Ph.D. Thesis, Ecole Polytechnique, Palaiseau, France.
5. Héripré, E., Dexet, M., Crépin, J., Gélébart, L., Roos, A., Bornert, M., Caldemaison, D. (2007) *Int. J. of Plasti.* **23**, 1512-1539.
6. Kabir, M.R., Chernova, L., Bartsch, M. (2010), *Acta Mater.* **58**, 5834-5847.
7. Roos, A., Chaboche, J.-L., Gélébart, L., Crépin, J. (2004), *Int. J. Plast.* **20**, pp. 811-830.
8. Roters, F., Eisenlohr, P., Hantcherli, L., Tjahjanto, D.D., Bieler, T.R., Raabe, D. (2010), *Acta Mat.* **58**, 1152-1211.
9. Simkin, B.A. Ph.D. Thesis (2003), Michigan State University, East Lansing, United States of America.
10. Werwer, M., Kabir, R., Cornec, A., Schwalbe, K.-H. (2007), *Eng. Frac. Mec.* **74**, 615-2638.
11. Fallahi, A., Mason, D., Kumar, D., Bieler, T.R., Crimp, M.A., *Mat. Sci. Engin.* **A432**, 281-291.
12. Simkin, B.A., Ng, B., Crimp, M.A., Bieler, T.R., (2007) *Intermet.* **15**, 55-60.
13. Geoffroy, D., Chiaruttini, V., Crépin, J., Héripré, E., Roos, A. (2011) CSMA 2011 10^e Colloque National en Calcul de Structures, Giens, France
14. St-Pierre, L., Héripré, E., Dexet, M., Crépin, J., Bertolino, G., Bilger, N. (2008) *Int. J. Plast.* **24**, 1516-153
15. Paul, J.D.H , Appel, F., Wagner, R. (1998), *Acta Mater.* **46**, 1075-1085.
16. Cailletaud, G. (1988) *Rev. Phys. App.* **23**, 353-363.
17. Cailletaud, G. Forest, S., Jeulin, D., Feyel, F., Galliet, I., Mounoury, V., Quilici, (2003) *S. Comp. Mat. Sc.* **27**, 351-374.
18. Gélébart, L. (2002) Ph.D. Thesis, Ecole Polytechnique, Palaiseau, France.
19. Tanaka, K., Ichitsubo, T., Inui, H., Yamaguchi, M., Koiwa, M. (1996) *Phil. Mag.* **73**, 71-78.
20. Lorentz, E. (2008) *Comput. Methods Appl. Mech. Engrg.* **198**, 302-317.
21. Mi, Y., Crisfield, M.A., Davies, G.A.O., Hellweg, H.B. (1998), *J. Compos. Mater.* **32**, 1246-1272.
22. Simkin, B.A., Ng, B., Crimp, M.A., Bieler, T.R., (2007) *Intermet.* **15**, 55-60.